Self-assembly of the tetrachlorido(oxalato)rhenate(iv) anion with protonated organic cations: X-ray structures and magnetic properties

Journal Name

ARTICLE

Self-assembly of the tetrachlorido(oxalato)rhenate(IV) anion with protonated organic cations: X-ray structures and magnetic properties

Received 00th January 2016,
Accepted 00th January 2016

DOI: 10.1039/x0xx00000x

www.rsc.org/

Anders H. Pedersen,[a] Miguel Julve,[b] Euan K. Brechin[a*] and José Martínez-Lillo[b*]

Two novel Re^{IV} compounds of formulae $[H_2bpy][Re^{IV}Cl_4(ox)]$ (**1**) and $[H_3biim]_2[Re^{IV}Cl_4(ox)]$ (**2**) [H_2bpy^{2+} = 4,4'-bipyridinium dication, H_3biim^+ = 2,2'-biimidazolium monocation, and ox = oxalate dianion] have been synthesised and magneto-structurally characterised. **1** crystallises in the monoclinic system with space group *C*2/*c*, and **2** crystallises in the triclinic system with space group $P\bar{1}$. The Re^{IV} ion in **1** and **2** is six-coordinate, bonded to four chloro ions and two oxalate-oxygen atoms in a distorted octahedral geometry. Short intermolecular Re^{IV}–Cl···Cl–Re^{IV} contacts, Cl···π type interactions and hydrogen bonds are present in the crystal lattice of both compounds, generating novel supramolecular structures based on the highly anisotropic $[Re^{IV}Cl_4(ox)]^{2-}$ species. Examination of the magnetic properties of **1** and **2** reveals significant antiferromagnetic coupling between Re^{IV} ions propagated primarily through the Re^{IV}–Cl···Cl–Re^{IV} interactions, as evidenced by the occurrence of maxima in the magnetic susceptibility at *ca*. 12 (**1**) and 17 K (**2**).

.

Introduction

The synthesis and development of new magnetic materials based on building blocks containing paramagnetic 4d and 5d metal ions is an emerging research topic in the field of molecular magnetism.[1-3] In comparison with 3d analogues, compounds involving 4d and 5d metal ions have been scarcely investigated, despite often exhibiting significantly stronger magnetic exchange interactions on account of their more diffuse magnetic orbitals. An illustrative example of this feature is provided by the relative magnitude of the ferromagnetic coupling across the oxalate bridge in the tetranuclear compounds $\{Cr[(\mu\text{-ox})Ni(Me_6\text{-}[14]ane\text{-}N_4)]_3\}(ClO_4)_3$ (Me_6-[14]ane-N_4 = (±)-5,7,7,12,14-hexamethyl-1,4,8,11-tetraazacyclotetradecane) where J = +5.3 cm^{-1},[4] and $(NBu_4)_4[\{ReCl_4(\mu\text{-ox})\}_3Ni]$ (NBu_4^+ = tetra-*n*-butylammonium cation and ox^{2-} = oxalate dianion) where J = +16.3 cm^{-1},[5,6] the Cr^{III} and Re^{IV} ions being isolectronic. Among the 5d metal ions, the paramagnetic Re^{IV} ion is very appealing to magnetochemists: it is a $5d^3$ metal ion whose ground electronic state is a $^4A_{2g}$ term with three unpaired electrons and a high value of the spin-orbit coupling constant (λ ≈ 1000 cm^{-1} in the free ion). The six-coordinate Re^{IV} possesses large magnetic anisotropy which arises from second order spin-orbit coupling; absolute values of the zero-field splitting parameter D ($2D$ is the energy gap between the two Kramers doublets M_S = ±3/2 and ±1/2) are generally in the range 9-26 cm^{-1} for the compounds $A_2[ReX_6]$ (A = univalent cation and X = F, Cl, Br and I),[7-28] and as large as 73 cm^{-1} for the compound $(NBu_4)_2[ReBr_4(ox)]$, which was recently reported as the first example of a 5d-based mononuclear Single-Ion Magnet (SIM).[29]

Because of the relatively large degree of spin delocalization that is spread from the Re^{IV} ion onto its coordinated ligands,[3,30-36] significant magnetic interactions can be mediated not only by bridging ligands in polynuclear compounds, but by intermolecular contacts, even at relatively large metal-metal distances. Typical pathways are of the type Re-X···X-Re,[7-28,31-33] Re-X···(H_2O)···X-Re[26,28] and Re-X···π···X-Re,[26,28] where X = halide anion.

As a continuation of our current research activity dealing with halorhenate(IV) salts aimed at analysing the nature and influence of such intermolecular interactions on magnetic properties, we herein report the synthesis and magneto-structural characterization of two novel Re^{IV} compounds based on the $[ReCl_4(ox)]^{2-}$ anion and of formulas $[H_2bpy][Re^{IV}Cl_4(ox)]$ (**1**) and $[H_3biim]_2[Re^{IV}Cl_4(ox)]$ (**2**) [H_2bpy^{2+} = 4,4'-bipyridinium dication and H_3biim^+ = 2,2'-biimidazolinium monocation].

A search of the literature and Cambridge Structural Database (CSD) reveals that 27 crystal structures containing the $[ReCl_4(ox)]^{2-}$ anion have been reported up to date. From them, only six are salts based on the non-coordinated $[ReCl_4(ox)]^{2-}$

[a] EaStCHEM School of Chemistry, The University of Edinburgh, David Brewster Road, EH9 3FJ Edinburgh, Scotland, United Kingdom.
[b] Instituto de Ciencia Molecular (ICMol), Universitat de València, C/Catedrático José Beltrán 2, 46980, Paterna, Valencia, Spain.

† Electronic Supplementary Information (ESI) available: Figures S1-S5. See DOI: 10.1039/x0xx00000x

anion and none contains protonated organic cations. The $[ReCl_4(ox)]^{2-}$ anion is a highly anisotropic complex that has been used as a precursor to build both discrete and 1D compounds, in many cases with pre-designed magnetic properties,[3] and there is no doubt that new magnetic systems will be obtained through intermolecular interactions driven by its chloride and oxalate groups, which can be very effective in crystal engineering.

Experimental section

Materials and physical measurements

All manipulations were performed under aerobic conditions, using materials as received (reagent grade). Tetra-n-butylammonium tetrachloro(oxalato)rhenate(IV), $(NBu_4)_2[ReCl_4(ox)]$, was prepared following the synthetic method described in the literature.[7]

Elemental analyses (C, H, N) were performed by MEDAC Ltd and by the Central Service for the Support to Experimental Research (SCSIE) at the University of Valencia. Infrared spectra of **1** and **2** were recorded with a PerkinElmer Spectrum 65 FT-IR (ATR device) spectrometer in the 4000-500 cm^{-1} region. Variable-temperature, solid-state direct current (dc) magnetic susceptibility data down to 2.0 K were collected on a Quantum Design MPMS-XL SQUID magnetometer equipped with a 7 T dc magnet. Experimental magnetic data were corrected for the diamagnetic contributions of the constituent atoms in **1** (-237.1 x 10^{-6} emu mol^{-1}) and in **2** (-264.2 x 10^{-6} emu mol^{-1}) by using Pascal's constants.[37,38]

Preparation of the compounds 1 and 2

Compound 1. $(NBu_4)_2[ReCl_4(ox)]$ (0.05 mmol, 45.0 mg) and 4,4'-bipyridine (0.20 mmol, 31.2 mg) were mixed and stirred for 2h in glacial acetic acid (3.0 mL). A yellow solid was obtained, collected by filtration, and recrystallized in hot 4 M HCl. Yellow crystals suitable for X-ray diffraction were grown by standing overnight in the fridge at 4 °C. Yield: 31%. Anal. Calc. (found) for $C_{12}H_{10}O_4N_2Cl_4Re$ (**1**): C, 25.1 (25.2); H, 1.8 (1.9); N, 4.9 (4.8) %. IR peaks (ATR/cm^{-1}): 3202(m), 3153(m), 3085(m), 1676(s), 1616(m), 1594(m), 1485(m), 1353(m), 1250(m), 1201(m), 993(m), 890(m), 799(s), 760(s).

Compound 2. $(NBu_4)_2[ReCl_4(ox)]$ (0.05 mmol, 45.0 mg) and 2,2'-biimidazole (0.10 mmol, 18.0 mg) were mixed in glacial acetic acid (4.0 mL). The solution was heated to 90 °C and stirred for 20 min. The resulting green solution was filtered while hot and left to evaporate at room temperature. Dark green crystals of **2** were grown in 1 week, which were suitable for X-ray diffraction studies. Yield: 42%. Anal. Calc. (found) for $C_{14}H_{14}O_4N_8Cl_4Re$ (**2**): C, 24.5 (24.6); H, 2.1 (2.0); N, 16.3 (16.2) %. IR peaks (ATR/cm^{-1}): 3147(w), 3128(m), 3043(m), 2951(m), 2825(w), 1712(vs), 1655(m), 1583(vs), 1429(w), 1321(m), 1207(m), 1115(m), 1087(m), 837(m), 657(m).

X-ray data collection and structure refinement

X-ray diffraction data on single crystals of dimensions 0.48 x 0.06 x 0.02 (**1**) and 0.43 x 0.35 x 0.06 mm^3 (**2**) were collected on a Bruker-Nonius X8APEXII CCD area detector diffractometer with graphite-monochromated Mo-K_α radiation (λ = 0.71073 Å). Crystal parameters and refinement results for **1** and **2** are summarized in Table 1. The structures of **1** and **2** were solved by direct methods and subsequently completed by Fourier recycling using OLEX2 (**1**)[39,40] and SHELXTL (**2**).[41-43] H(2) in **1** and H(2a), H(3a), H(4a), H(6a), H(7a) and H(8a) in **2** were seen in the difference maps before they were geometrically created in the model. The final full-matrix least-squares refinements on F^2, minimising the function $\sum w(|F_o|-|F_c|)^2$, reached convergence with the values of the discrepancy indices given in Table 1. The graphical manipulations were performed with the DIAMOND program.[44] CCDC 1503662 (**1**) and 1503663 (**2**).

Table 1. Summary of the crystal data and structure refinement parameters for 1 and 2

Compound	**1**	**2**
Formula	$C_{12}H_{10}N_2O_4Cl_4Re$	$C_{14}H_{14}N_8O_4Cl_4Re$
M_r/g mol^{-1}	574.22	686.33
Crystal system	monoclinic	triclinic
Space group	$C2/c$	$P\bar{1}$
a/Å	9.307(1)	9.864(1)
b/Å	17.627(1)	9.991(1)
c/Å	10.807(1)	12.136(1)
α/°	90	93.36(1)
β/°	113.59(1)	92.33(1)
γ/°	90	119.54(1)
V / Å^3	1624.8(1)	1035.51(3)
Z	4	2
D_c/g cm^{-3}	2.347	2.201
μ(Mo-K_α)/mm^{-1}	20.879	6.426
F(000)	1084	658
Goodness-of-fit on F^2	1.032	1.006
R_1 [$I > 2\sigma(I)$]	0.0322	0.0167
wR_1 [$I > 2\sigma(I)$]	0.0849	0.0458
$\Delta\rho_{max, min}$/e Å^{-3}	2.790 and -1.230	0.914 and -1.049

Results and discussion

Synthesis. Compounds **1** and **2** were synthesised from tetra-*n*-butylammonium tetrachloro(oxalato)rhenate(IV) in glacial CH_3COOH (**1** and **2**) and 4 M HCl (1) solutions in the presence of 4,4'-bipyridine (**1**) and 2,2'-biimidazole (**2**), which were

protonated *in situ*. While crystals of **1** are obtained by standing overnight in the fridge at 4 °C, those of **2** were grown in one week after slow evaporation of the mother liquor at room temperature. It is worth noting that the oxalate dianion remains coordinated to the Re^{IV} metal ion and undergoes neither protonation nor dissociation, a feature which is quite unusual under such reaction conditions.

Structure Description of 1 and 2

Compound **1** crystallises in the monoclinic system with space group *C*2/c, and compound **2** crystallises in the triclinic system with space group *P*$\bar{1}$ (Table 1). Their structures are made up of $[ReCl_4(ox)]^{2-}$ anions (**1** and **2**) and diprotonated $[H_2bpy]^{2+}$ (**1**) and monoprotonated $[H_3biim]^{+}$ (**2**) cations which self-assemble through an extended network of hydrogen bonds, Cl···Cl and Cl···π type intermolecular interactions.

The asymmetric unit in **1** consists of two chloride ions, half an oxalate molecule, half a 4,4'-bipyridinium cation, together with a rhenium ion that lies on a special position (Fig. 1). Two $[H_3biim]^{+}$ cations and one $[ReCl_4(ox)]^{2-}$ anion form the asymmetric unit in **2** (Fig. 2).

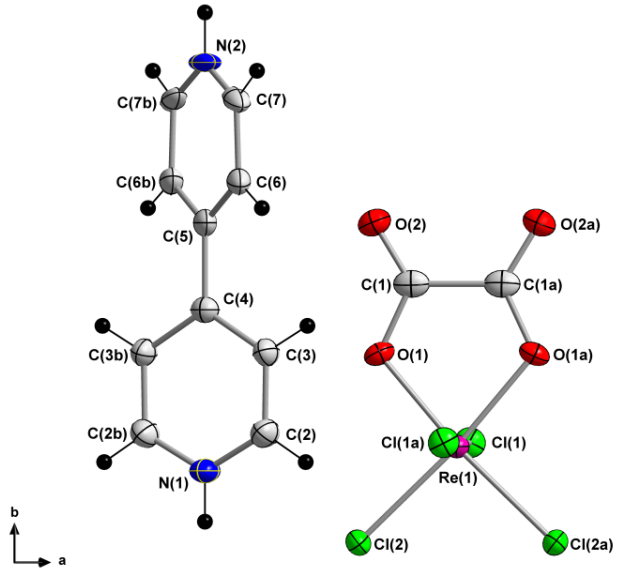

Fig. 1. Molecular structure of the diprotonated $[H_2bpy]^{2+}$ cation and the $[ReCl_4(ox)]^{2-}$ anion in **1**. Thermal ellipsoids are depicted at the 50% probability level [Symmetry code: (a) = -*x*, *y*, -*z*+1/2; (b) = -*x*-1, *y*, -*z*-1/2].

Each Re^{IV} ion in **1** and **2** is six-coordinate and bonded to four chloride ions and two oxalate-oxygen atoms in a distorted octahedral geometry. The small bite angle of the oxalate is the main source of this distortion, the value of the angle subtended by this ligand at the rhenium ion is 80(1)° [O(1)–Re(1)–O(1a), (a) = -*x*, *y*, -*z*+1/2] and 79(1)° [O(1)–Re(1)–O(4)] for **1** and **2**, respectively. The Re-Cl and Re-O bond lengths [Re(1)-Cl(1) = 2.344(1) Å, Re(1)-Cl(2) = 2.337(1) Å, and Re(1)-O(1) = 2.051(1) Å in **1**, and average values of Re-Cl = 2.335(1) Å and Re-O = 2.057(1) Å in **2**] are similar in both compounds and are in agreement with those of previously reported compounds based on the anionic $[ReCl_4(ox)]^{2-}$ entity.[45-54]

Table 2. Hydrogen-Bonding Interactions in 1[a]

D-H···A	D-H/Å	H···A/Å	D···A/Å	(DHA)/°
N(1)-H(1)···Cl(2a)	0.880	2.54(1)	3.242(1)	138.8(1)
N(1)-H(1)···Cl(2b)	0.880	2.54(1)	3.242(1)	138.8(1)
N(2)-H(2)···O(2c)	0.880	2.17(1)	2.869(1)	139.9(1)
N(2)-H(2)···O(2d)	0.880	2.17(1)	2.869(1)	139.9(1)

[a]Symmetry codes: (a) = -*x*-1/2, -*y*+1/2, -*z*; (b) = *x*-1/2, -*y*+1/2, *z*-1/2; (c) = -*x*-1/2, -*y*+3/2, -*z*; (d) = *x*-1/2, -*y*+3/2, *z*-1/2.

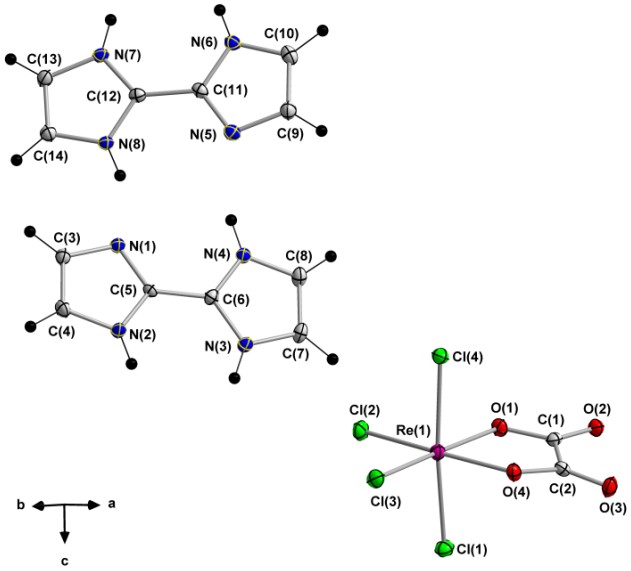

Fig. 2. Molecular structure of the monoprotonated $[H_3biim]^{+}$ cations and the $[ReCl_4(ox)]^{2-}$ anion in **2**. Thermal ellipsoids are depicted at the 50% probability level.

Table 3. Hydrogen-Bonding Interactions in 2[a]

D-H···A	D-H/Å	H···A/Å	D···A/Å	(DHA)/°
N(2)-H(2)···O(1a)	0.880	2.07(1)	2.932(1)	167.8(1)
N(3)-H(3)···O(2a)	0.880	2.00(1)	2.830(1)	156.8(1)
N(4)-H(4)···N(5)	0.880	2.00(1)	2.841(1)	158.5(1)
N(8)-H(8)···N(1)	0.880	1.92(1)	2.745(1)	155.6(1)
N(6)-H(6)···O(3b)	0.880	2.08(1)	2.877(1)	151.0(1)
N(7)-H(7)···O(4b)	0.880	2.07(1)	2.923(1)	163.9(1)

[a]Symmetry codes: (a) = *x*, *y*+1, *z*; (b) = *x*-1, *y*, *z*-1.

The 4,4'-bipyridinium cation in **1** exhibits protonation on both nitrogen atoms [N(1) and N(2)], with the two pyridyl rings being non coplanar, the torsion angle through the inter-ring carbon–carbon bond [C(3)-C(4)-C(5)-C(6b), (b) = -*x*-1, *y*, -*z*-1/2] is approximately 148° (Fig. 1). The average values of the C–C and C–N bond lengths are in agreement with those found in salts based on this doubly protonated organic cation.[55-61]

In the crystal of **1**, the $[ReCl_4(ox)]^{2-}$ anions sit between two $[H_2bpy]^{2+}$ cations, being linked alternately by bifurcated N-H···$(O)_2$ and N-H···$(Cl)_2$ three-centered hydrogen bonds [the values of the N···O and N···Cl distances being *ca*. 2.87 Å and *ca*. 3.24 Å, respectively] (Table 2).[62-63] This leads to a chain-like motif growing along the crystallographic *b* axis (Figure 3).

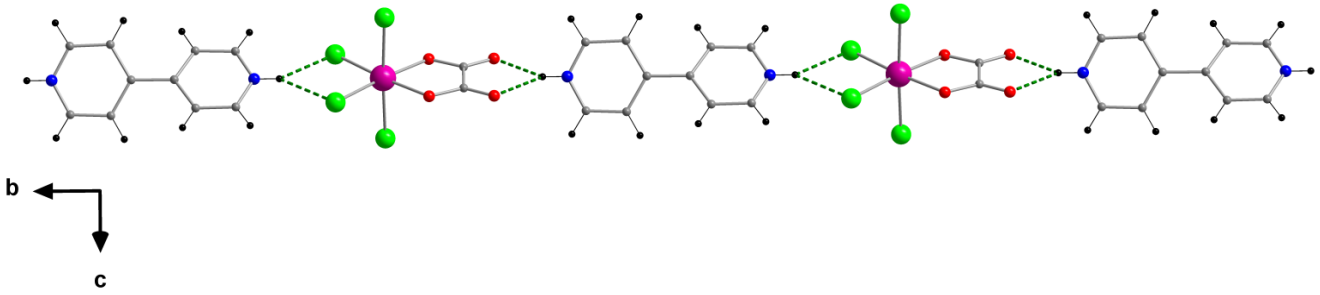

Fig. 3. View of the one-dimensional motif generated by bifurcated three-centered hydrogen bonds between the $[H_2bpy]^{2+}$ organic cations and $[ReCl_4(ox)]^{2-}$ anions in the crystal of **1** (dashed green lines). Colour code: pink, Re; green, Cl; red, O; blue, N; grey, C; black, H.

Further C-H···Cl type interactions between $[H_2bpy]^{2+}$ cations and $[ReCl_4(ox)]^{2-}$ anions of adjacent chains lead to the formation of a two-dimensional supramolecular network in the crystal structure of **1** (Fig. 4). In addition, short Cl···Cl contacts of 3.698(2) Å [Cl(2)···Cl(2c), (c) = -*x*-1/2, -*y*+1/2, -*z*] between $[ReCl_4(ox)]^{2-}$ anions generate anionic chains which grow along the crystallographic [101] direction (Fig. S1). Additional longer Cl···Cl interactions of 3.959(1) Å [Cl(1)···Cl(1d), (d) = -*x*, -*y*+1, -*z*] results in an anionic layered structure in **1** (Fig. 5). The shortest Re···Re separation is 6.720(1) Å [Re(1)···Re(1d)]. These 2D networks are tied together into the overall three-dimensional structure through C–H···Y (Y = Cl and O) and Cl···π contacts with distances of ≥ 3.32 Å (Fig. S2).

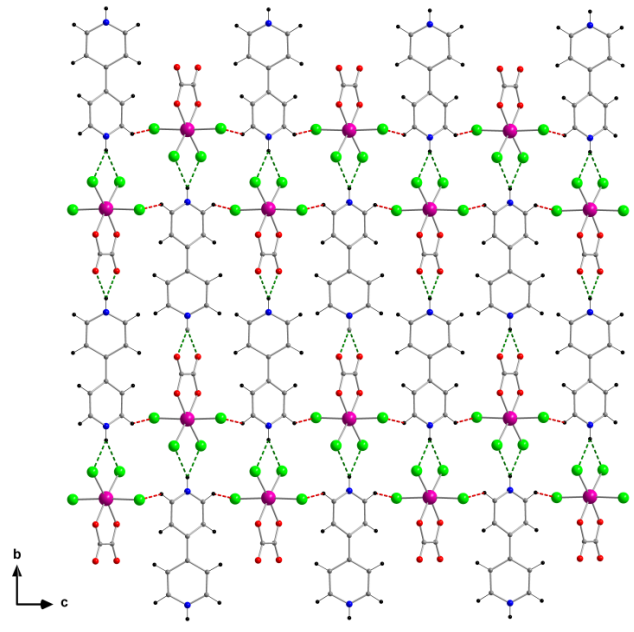

Fig. 4. Perspective view of the supramolecular two-dimensional arrangement of $[H_2bpy]^{2+}$ cations and $[ReCl_4(ox)]^{2-}$ anions of **1** through N-H···Cl and N-H···O hydrogen bonds (dashed green lines) and C-H···Cl type intermolecular interactions (dashed red lines). Colour code: pink, Re; green, Cl; red, O; blue, N; grey, C; black, H.

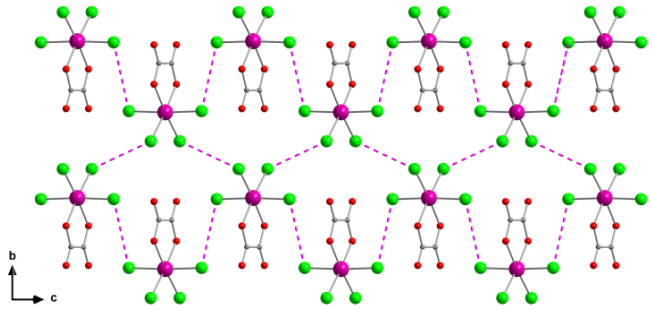

Fig. 5. View of a fragment of the crystal packing of **1** through the bc plane, showing an anionic layer connected by Cl···Cl contacts (dashed lines). Colour code: pink, Re; green, Cl; red, O; blue, N; grey, C; black, H.

Two crystallographically independent monoprotonated 2,2'-biimidazolium cations charge balance the $[ReCl_4(ox)]^{2-}$ unit in the structure of **2**. The protonation involves the N(3) and N(7) atoms (see Fig. 2). In both cases, the two imidazole rings are essentially coplanar. The average C–C and C–N bond length values agree with those found in previously reported salts containing this monoprotonated organic cation.[64-68]

In the crystal packing of **2**, H-bonded pairs of $[H_3biim]^{+}$ cations [the shortest N···N distance being *ca*. 2.75 Å] intercalate between the $[ReCl_4(ox)]^{2-}$ anions linking them into chains by means of N-H···O hydrogen-bonding interactions [the shortest N···O distance being *ca*. 2.83 Å] (see Figure 6 and Table 3). As seen in **1**, short Cl···Cl contacts of 3.507(1) Å [Cl(4)···Cl(4a), (a) = -*x*+2, -*y*+1, -*z*+1] and 3.987(1) Å [Cl(1)···Cl(1b), (b) = -*x*+2, -*y*+1, -*z*+2] between $[ReCl_4(ox)]^{2-}$ anions direct anionic chains, which grow along the crystallographic *c* axis (see Fig. S3). The shortest Re···Re separation in **2** is 6.414(1) Å [Re(1)···Re(1a)].

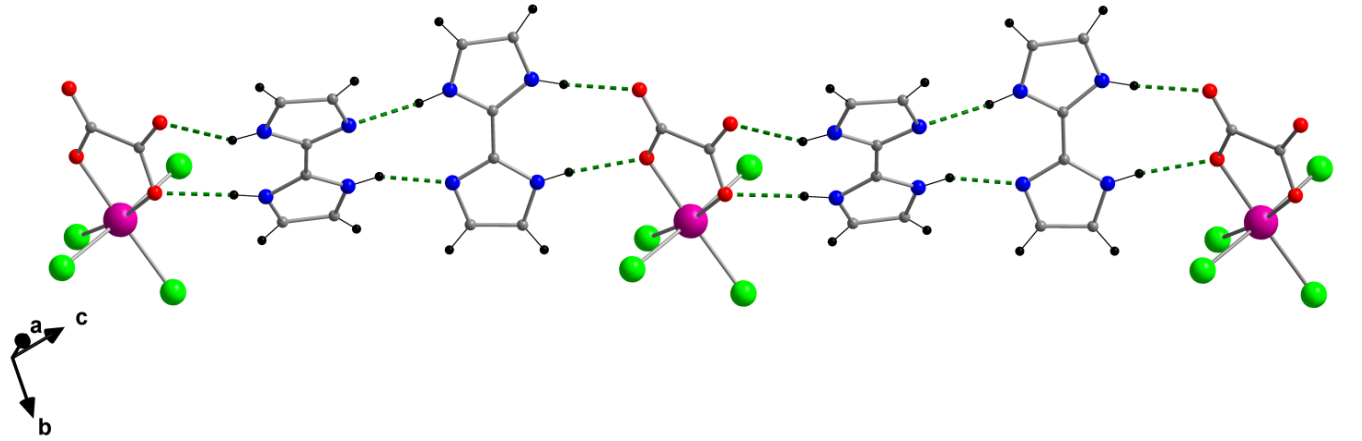

Fig. 6. View of the one-dimensional arrangement of $[H_3biim]^+$ cations and $[ReCl_4(ox)]^{2-}$ anions in **2** mediated through N-H···O and N-H···N hydrogen bonding interactions between anions and cations and pairs of cations, respectively (dashed lines). Colour code: pink, Re; green, Cl; red, O; blue, N; grey, C; black, H.

These chains are connected together into sheets of $[H_3biim]^+$ cations and $[ReCl_4(ox)]^{2-}$ anions *via* a series of C–H···Y (Y = Cl and O) intermolecular interactions (Fig. 7). The sheets propagate along the crystallographic [111] direction (Fig. S4) and are separated from each other by C–H···Cl, C–H···O, and Cl···π [distances of ≥ 3.69 Å] supramolecular interactions (Fig. S5).

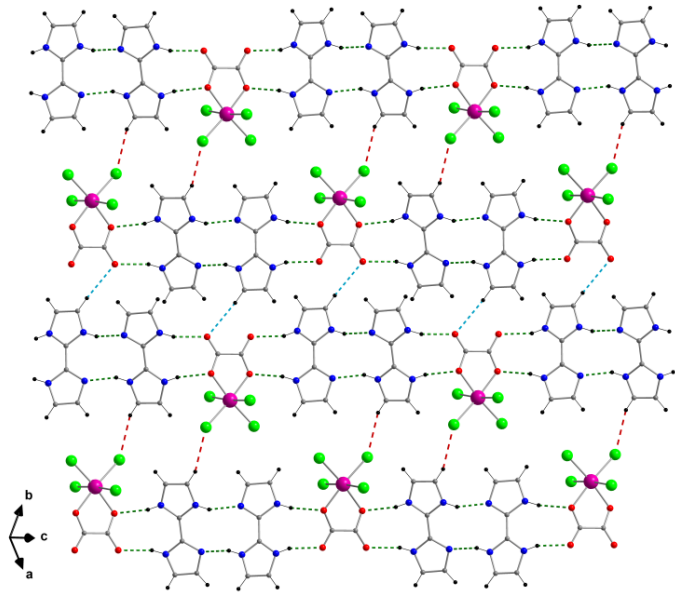

Fig. 7. Perspective view of the supramolecular 2D assembly of $[H_3biim]^+$ cations and $[ReCl_4(ox)]^{2-}$ anions of **2** through H-bonds (dashed green lines), and C–H···Cl (dashed red lines), and C–H···O type interactions (dashed blue lines). Colour code: pink, Re; green, Cl; red, O; blue, N; grey, C; black, H.

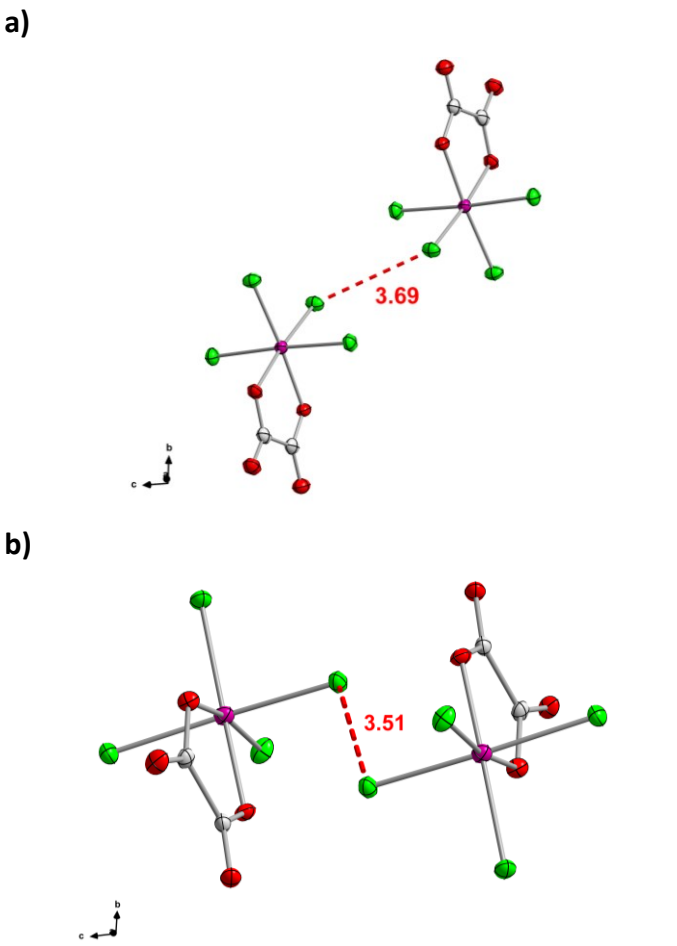

Fig. 8. Detail of the shortest Cl···Cl distance (in Å) connecting $[ReCl_4(ox)]^{2-}$ anions in **1** (**a**) and **2** (**b**) (dashed red lines). Colour code: pink, Re; green, Cl; red, O; grey, C.

Magnetic properties

Dc magnetic susceptibility measurements were performed on microcrystalline samples of **1** and **2** in the 2.0-300 K temperature range, under an external magnetic field of 0.1 T. The magnetic properties of **1** and **2** in the form of both $\chi_M T$ and χ_M *vs*. *T* plots (χ_M being the molar magnetic susceptibility) are shown in Figures 9 and 10, respectively. Similar magnetic behaviour is observed for both compounds. At room temperature, the $\chi_M T$ value is 1.53 $cm^3\ mol^{-1}\ K$ (**1** and **2**), a value which is very close to that expected for a magnetically isolated Re^{IV} (S_{Re} = 3/2) mononuclear complex with *g* = 1.8–1.9.[3] Upon cooling, the $\chi_M T$ values for **1** and **2** continuously decrease and practically vanish at very low temperatures reaching values of 0.03 (**1**) and 0.02 $cm^3\ mol^{-1}\ K$ (**2**) at 2.0 K. The decrease of $\chi_M T$ observed for **1** and **2** is likely due to the presence of intermolecular interactions and/or zero-field splitting (zfs) effects.[3,7-36]

The presence of a maximum in the magnetic susceptibility at *ca*. 12.0 (**1**) and 17.0 K (**2**) (see insets of Figs. 9 and 10) unambiguously supports the occurrence of antiferromagnetic exchange interactions between the Re^{IV} ions. No out-of-phase signals in the *ac* magnetic susceptibility are observed for either **1** or **2**. This is in contrast to that previously seen and studied for the parent compound $(NBu_4)_2[ReCl_4(ox)]$, that exhibits single-ion magnet (SIM) behaviour.[29]

A detailed inspection of the crystal packing of **1** and **2** reveals the existence of short Cl···Cl contacts between the paramagnetic $[ReCl_4(ox)]^{2-}$ anions in their crystal lattices (Fig. 8). Hence, the presence of relatively important through-space interactions between the spin carriers precludes the occurrence of SIM behaviour.

In order to analyze the magnetic behaviour of **1** and **2**, we have employed the Hamiltonian of equation (1) and its derived theoretical expression for the magnetic susceptibility, equation (2),[69] by including a θ term (as *T*-θ) to account for the observed intermolecular interactions.

$$\hat{H} = D\left[(\hat{S}_z)^2 - S(S+1)/3\right] + g\beta H\hat{S} \quad (1)$$

$$\chi_M = \frac{\chi_{//} + 2\chi_{\perp}}{3} \quad (2)$$

$$\chi_{//} = \frac{N\beta^2 g_{//}^2}{4k(T-\theta)} \frac{1+9\exp(-2D/kT)}{1+\exp(-2D/kT)}$$

$$\chi_{\perp} = \frac{N\beta^2 g_{\perp}^2}{k(T-\theta)} \frac{1+(3kT/4D)\left[1-\exp(-2D/kT)\right]}{1+\exp(-2D/kT)}$$

The first term in equation (1) corresponds to the zero-field splitting and the second term the Zeeman effects.

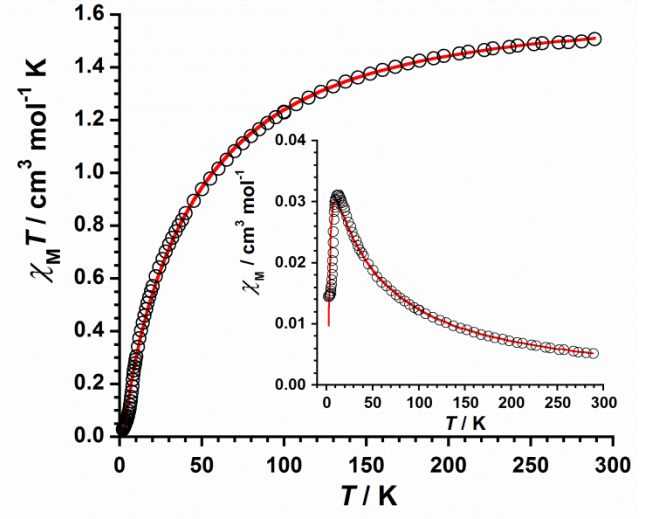

Fig. 9. Thermal variation of the $\chi_M T$ product for **1**. The solid red line represents the best-fit of the experimental data (see text). The inset shows the temperature dependence of the magnetic susceptibility.

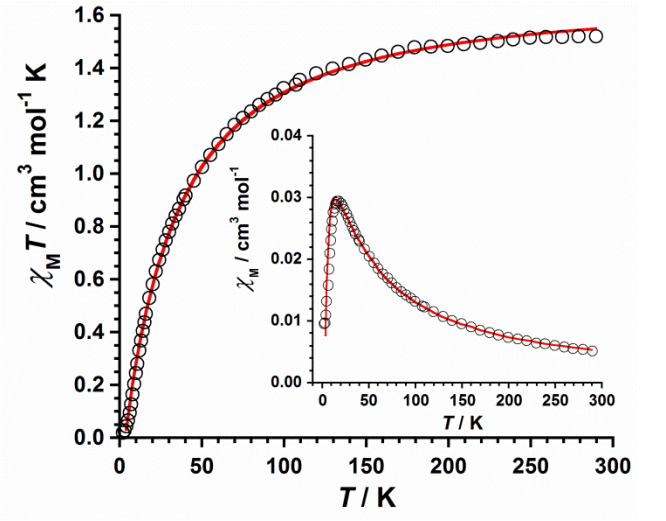

Fig. 10. Thermal variation of the $\chi_M T$ product for **2**. The solid red line represents the best-fit of the experimental data (see text). The inset shows the temperature dependence of the magnetic susceptibility.

HF-EPR and theoretical studies performed on the $[ReCl_4(ox)]^{2-}$ moiety, prepared as a magnetically isolated salt, supports a value of *D* = -53 cm^{-1} for this unit.[29] Thus, *D* was kept constant during the fitting process. The resulting best least-squares fit parameters, represented as solid red lines in Figures 9 and 10, are *g* = 1.88 and θ = - 14.7 K with *R* = 6.8 x 10^{-5} for **1**, and *g* = 1.89 and θ = - 18.4 K with *R* = 1.3 x 10^{-4} for **2** {*R* being the agreement factor defined as $\Sigma_i[(\chi_M T)_i^{obs} - (\chi_M T)_i^{calc}]^2 / [(\chi_M T)_i^{obs}]^2$}.

The *g* values calculated for **1** and **2** are in agreement with those previously reported for mononuclear Re^{IV} complexes.[3,7-

[36] The negative values of θ confirm the presence of relatively strong antiferromagnetic exchange through intermolecular Re-Cl···Cl-Re pathways (see Fig. 8), with the shorter interactions in **2** resulting in stronger exchange.

Conclusions

In summary, the crystal structures and magnetic properties of two novel Re^{IV} compounds based on the $[ReCl_4(ox)]^{2-}$ anion and protonated organic cations, of formulae $[H_2bpy][ReCl_4(ox)]$ (**1**) and $[H_3biim]_2[ReCl_4(ox)]$ (**2**) [H_2bpy^{2+} = 4,4'-bipyridinium dication and H_3biim^+ = 2,2'-biimidazolinium monocation], have been studied for the first time. In both compounds the molecules self-assemble into novel supramolecular structures through a variety of intermolecular interactions including hydrogen bonds and Re-Cl···Cl-Re contacts. The latter are responsible for propagating relatively strong antiferromagnetic exchange interactions between the anions.

Acknowledgements

Financial support from the Spanish Ministry of Economy and Competitiveness (MINECO) (projects CTQ2013-44844P and CTQ2016-75068P) and the Excellence Unit "María de Maeztu" (project MDM-2015-0538) is gratefully acknowledged. EKB thanks the EPSRC. JML thanks the Spanish MINECO for a "Ramon y Cajal" grant. The authors thank Dr. Gary Nichol for single-crystal X-ray diffraction measurements.

Notes and references

1. X.-Y. Wang, C. Avendaño and K. R. Dunbar, *Chem. Soc. Rev*. 2011, **40**, 3213–3238.
2. D. Pinkowicz, R. Podgajny, B. Nowicka, S. Chorazy, M. Reczyński and B. Sieklucka, *Inorg. Chem. Front.* 2015, **2**, 10-27.
3. J. Martínez-Lillo, J. Faus, F. Lloret and M. Julve, *Coord. Chem. Rev*. 2015, **289–290**, 215–237
4. Y. Pei, Y. Journaux and O. Kahn, *Inorg. Chem.* 1989, **28**, 100-103.
5. J. Martínez-Lillo, D. Armentano, G. De Munno, W. Wernsdorfer, M. Julve, F. Lloret and J Faus, *J. Am. Chem. Soc.* 2006, **128**, 14218-14219.
6. J. Martínez-Lillo, D. Armentano, G. De Munno, W. Wernsdorfer, J. M. Clemente-Juan, J. Krzystek, F. Lloret, J. Julve and J. Faus, *Inorg. Chem.* 2009, **48**, 3027-3038.
7. R. Chiozzone, R. González, C. Kremer, G. De Munno, J. Cano, F. Lloret, M. Julve and J. Faus, *Inorg. Chem.* 1999, **38**, 4745-4752.
8. A. Tomkiewicz, F. Villain and J. Mroziński, *J. Mol. Struct.* 2000, **555**, 383-390.
9. R. González, R. Chiozzone, C. Kremer, G. De Munno, F. Nicolò, F. Lloret, M. Julve and J. Faus, *Inorg. Chem.* 2003, **42**, 2512-2518.
10. R. González, R. Chiozzone, C. Kremer, F. Guerra, G. De Munno, F. Lloret, M. Julve and J. Faus *Inorg. Chem.* 2004, **43**, 3013-3019.
11. M. Holynska, M. Korabik and T. Lis *Acta Crystallogr.* 2006, **E62**, m3178-m3180.
12. K. S. Pedersen, M. Sigrist, M. A. Sørensen, A.-L. Barra, T. Weyhermüller, S. Piligkos, C. A. Thuesen, M. G. Vinum, H. Mutka, H. Weihe, R. Clérac and J. Bendix, *Angew. Chem. Int. Ed*. 2014, **53**, 1351-1354.
13. P. A. Reynolds, B. Moubaraki, K. S. Murray, J. W. Cable, L. M. Engelhardt and B. N. Figgis, *J. Chem. Soc., Dalton Trans.* 1997, 263-268.
14. P. A. Reynolds, B. N. Figgis and D. Martin y Marero, *J. Chem. Soc., Dalton Trans.* 1999, 945-950.
15. J. Martínez-Lillo, J. Kong, W. P. Barros, J. Faus, M. Julve and E. K. Brechin, *Chem. Commun*., 2014, **50**, 5840.
16. R. H. Busey and E. Sonder, *J. Chem. Phys.* 1962, **36**, 93-97.
17. R. H. Busey, H. H. Dearman and R. B. Jr. Bevan, *J. Phys. Chem.* 1962, **66**, 82-89.
18. V. Minkiewicz, G. Shirane, B. Frazer, R. Wheeler and J. Dorain, *Phys. Chem. Solids* 1968, **29**, 881-884.
19. J. Mroziński, *Bull. Acad. Pol. Sci., Ser. Sci. Chim*., 1978, **26**, 789-798.
20. J. Martínez-Lillo, D. Armentano, G. De Munno, F. Lloret, M. Julve and J. Faus, *Cryst. Growth Des.* 2006, **6**, 2204-2206.
21. J. Martínez-Lillo, D. Armentano, N. Marino, L. Arizaga, R. Chiozzone, R. González, C. Kremer, J. Cano and J. Faus, *Dalton Trans*. 2008, 4585-4594.
22. K. I. Suzuki, T. Kodama, K. Kikuchi and W. Fujita, *Chem. Lett*., 2010, **39**, 1096-1098.
23. D. Armentano and J Martínez-Lillo, *Inorg. Chim. Acta.* 2012, **380**, 118-124.
24. F. Pop, M. Allain, P. Auban-Senzier, J. Martínez-Lillo, F. Lloret, M. Julve, E. Canadell and N. Avarvari, *Eur. J. Inorg. Chem*. 2014, 3855-3862.
25. J. Martínez-Lillo, *Polyhedron*, 2014, **67**, 213-217.
26. J. Martínez-Lillo, D. Armentano, G. De Munno, N. Marino, F. Lloret, M. Julve and J. Faus, *CrystEngComm*, 2008, **10**, 1284-1287.
27. J. Martínez-Lillo, J. Kong, M. Julve and E. K. Brechin, *Cryst. Growth Des*. 2014, **14**, 5985-5990.
28. J. Martínez-Lillo, A. H. Pedersen, J. Faus, M. Julve and E. K. Brechin, *Cryst. Growth Des.* 2015, **15**, 2598-2601.
29. J. Martínez-Lillo, T. F. Mastropietro, E. LHotel, C. Paulsen, J. Cano, G. De Munno, J. Faus, F. Lloret, M. Julve, S. Nellutla and J. Krzystek *J. Am. Chem. Soc.* 2013, **135**, 13737-13748.
30. A. Cuevas, R. Chiozzone, C. Kremer, L. Suescun, A. Mombrú, D. Armentano, G. De Munno, F. Lloret, J. Cano, and J. Faus, *Inorg. Chem.* 2004, **43**, 7823-7831.
31. J. Martínez-Lillo, D. Armentano, G. De Munno and J. Faus, *Polyhedron*. 2008, **27**, 1447-1454.
32. J. Martínez-Lillo, F. Lloret, M. Julve and J. Faus, *J. Coord. Chem.* 2009, **62**, 92-99.
33. J. Martínez-Lillo, D. Armentano, T. F. Mastropietro, M. Julve, J. Faus and G. De Munno, *Cryst. Growth Des.* 2011, **11**, 1733-1741.
34. J. Martínez-Lillo, L. Cañadillas-Delgado, J. Cano, F. Lloret, M. Julve and J. Faus, *Chem. Commun*. 2012, **48**, 9242–9244.
35. J. Martínez-Lillo, D. Armentano, G. De Munno, M. Julve, F. Lloret and J. Faus, *Dalton Trans.* 2013, **42**, 1687-1695.
36. J. Martínez-Lillo, J. Cano, W. Wernsdorfer and E. K. Brechin, *Chem. - Eur. J*. 2015, **21**, 8790–8798.

37. A. Earnshaw, *Introduction to Magnetochemistry*, Academic Press, London, Kahn, 1968.
38. G. A. Bain and J. F. Berry, *J. Chem. Educ*., 2008, **85**, 532-536.
39. O. V. Dolomanov, L. J. Bourhis, R. J. Gildea, J. A. K. Howard and H. Puschmann, *J. Appl. Cryst*. 2009, **42**, 339-341.
40. L. J. Bourhis, O. V. Dolomanov, R. J. Gildea, J. A. K. Howard, H. Puschmann, *Acta Cryst*. 2015, **A71**, 59-75.
41. G. M. Sheldrick, *Acta Cryst*. 2008, **A64**, 112.
42. G. M. Sheldrick, *Acta Cryst*. 2015, **C71**, 3-8.
43. SHELXTL; Bruker Analytical X-ray Instruments: Madison, WI, 1998.
44. DIAMOND 3.2d, Crystal Impact GbR, CRYSTAL IMPACT; K. Bra
45. A. Tomkiewicz, T. J. Bartczak, R. Kruszyński and J. Mroziński, *J. Mol. Struct*. 2001, **595**, 225-231.
46. A. Tomkiewicz, J. Mroziński, I. Brüdgam and H. Hartl, *Eur. J. Inorg. Chem*. 2005, 1787–1793.
47. S. Benmansour, E. Coronado, C. Giménez-Saiz, C. Gómez-García and C. Rößer, *Eur. J. Inorg. Chem*. 2014, 3949-3959.
48. R. Chiozzone, R. González, C. Kremer, G. De Munno, D. Armentano, F. Lloret, M. Julve and J. Faus, *Inorg. Chem*. 2003, **42**, 1064–1069.
49. J. Martínez-Lillo, F. S. Delgado, C. Ruiz-Pérez, F. Lloret, M. Julve and J. Faus, *Inorg. Chem*. 2007, **46**, 3523-3530.
50. A. Bieńko, J. Kłak, J. Mroziński, R. Kruszyński, D. C. Bieńko and R. Boča, *Polyhedron* 2008, **27**, 2464-2470.
51. A. Bieńko, R. Kruszyński and D. Bieńko, *Polyhedron* 2014, **75**, 1-8.
52. J. Martínez-Lillo, D. Armentano, G. De Munno, F. Lloret, M. Julve and J. Faus, *Dalton Trans*. 2008, 40-43.
53. J. Martínez-Lillo, D. Armentano, G. De Munno, F. Lloret, M. Julve and J. Faus, *Dalton Trans*. 2011, **40**, 4818-4820.
54. D. Armentano and J. Martínez-Lillo, *Cryst. Growth Des*. 2016, **16**, 1812–1816.
55. A. L. Gillon, A. G. Orpen, J. Starbuck, X.-M. Wang, Y. Rodríguez-Martín and C. Ruiz-Pérez, *Chem. Commun*., 1999, 2287–2288.
56. C. Ruiz-Pérez, P. Lorenzo-Luis, M. Hernández-Molina, M. M. Laz, P. Gili and M. Julve, *Cryst. Growth Des.* 2004, **4**, 57-61.
57. O. Fabelo, L. Cañadillas-Delgado, F. S. Delgado, P. Lorenzo-Luis, M. Laz, M. Julve and C. Ruiz-Pérez, *Cryst. Growth Des.* 2005, **5**, 1163-1167.
58. R. D. Willett, R. E. Butcher, Ch. P. Landee and B. Twamley, *Polyhedron* 2006, **25**, 2093–2100.
59. H. Kumagai and S. Kawata *Acta Cryst.* 2011, **E67**, o2636.
60. H. Lu, R. Gautier, M. D. Donakowski, Z. Liu and K. R. Poeppelmeier, *Inorg. Chem.* 2014, **53**, 537−542.
61. S. K. Dey, R. Saha, S. Biswas, A. Layek, S. Middya, I. M. Steele, M. Fleck, P. P. Ray and S. Kumar, *Cryst. Growth Des*. 2014, **14**, 207−221.
62. G. A. Jeffrey, *Cryst. Rev*. 1995, **4**, 213-254.
63. I. Rozas, I. Alkorta and J. Elguero, *J. Phys. Chem*. *A* 1998, **102**, 9925-9932.
64. K. Ramírez, J. A. Reyes, A. Briceño and R. Atencio, *CrystEngComm*, 2002, **4**, 208–212.
65. S. Lie, T. Maris, C. Malveau, D. Beaudoin, F. Helzy and J. D. Wuest, *Cryst. Growth Des*. 2013, **13**, 1872−1877.
66. X.-L. Gao, L.-F. Bian and S.-W. Guo, *Acta Cryst.* 2014, **E70**, o1221–o1222.
67. Y.-B. Lu, F.-M. Jian, S. Jin, J.-W. Zhao, Y.-R. Xie and G.-T. Luo, *Cryst. Growth Des*., 2014, **14**, 1684–1694.
68. Z.-L. Li, Y. Wang, L.-C. Zhang, J.-P. Wang, W.-S. You and Z.-M. Zhu, *Dalton Trans*., 2014, **43**, 5840-5846.
69. O. Kahn, *Molecular Magnetism*; VCH: New York, 1993.